

The “Somersault” Mechanism for the P-450 Hydroxylation of Hydrocarbons. The Intervention of Transient Inverted Metastable Hydroperoxides

Robert D. Bach* and Olga Dmitrenko

Contribution from the Department of Chemistry and Biochemistry, University of Delaware, Newark, Delaware 19716

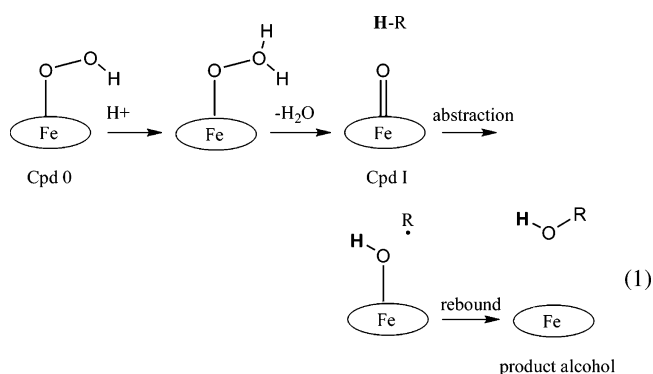
Received April 2, 2005; E-mail: rbach@udel.edu

Abstract: A series of model theoretical calculations are described that suggest a new mechanism for the oxidation step in enzymatic cytochrome P450 hydroxylation of saturated hydrocarbons. A new class of metastable metal hydroperoxides is described that involves the rearrangement of the ground-state metal hydroperoxide to its inverted isomeric form with a hydroxyl radical hydrogen bonded to the metal oxide ($\text{MO}-\text{OH} \rightarrow \text{MO}\cdots\text{HO}$). The activation energy for this somersault motion of the $\text{FeO}-\text{OH}$ group is 20.3 kcal/mol for the P450 model porphyrin iron(III) hydroperoxide [$\text{Por}(\text{SH})\text{Fe}(\text{III})-\text{OOH}^-$] to produce the isomeric ferryl oxygen hydrogen bonded to an $\bullet\text{OH}$ radical [$\text{Por}(\text{SH})\text{Fe}(\text{III})-\text{O}\cdots\text{HO}^-$]. This isomeric metastable hydroperoxide, the proposed primary oxidant in the P450 hydroxylation reaction, is calculated to be 17.8 kcal/mol higher in energy than the ground-state iron(III) hydroperoxide Cpd 0. The first step of the proposed mechanism for isobutane oxidation is abstraction of a hydrogen atom from the C–H bond of isobutane by the hydrogen-bonded hydroxyl radical to produce a water molecule strongly hydrogen bonded to anionic Cpd II. The hydroxylation step involves a concerted but nonsynchronous transfer of a hydrogen atom from this newly formed, bound, water molecule to the ferryl oxygen with a concomitant rebound of the incipient $\bullet\text{OH}$ radical to the carbon radical of isobutane to produce the C–O bond of the final product, *tert*-butyl alcohol. The TS for the oxygen rebound step is 2 kcal/mol lower in energy than the hydrogen abstraction TS ($\Delta E^\ddagger = 19.5$ kcal/mol). The overall proposed new mechanism is consistent with a lot of the ancillary experimental data for this enzymatic hydroxylation reaction.

1. Introduction

Members of the cytochrome P450 monooxygenase family play vital roles in the synthesis and degradation of many physiologically important compounds and xenobiotics.¹ Cytochrome P-450 enzymes catalyze a diversity of oxidations, including such normally difficult reactions as the hydroxylation of hydrocarbons; such reactions should require a high-energy reactant. The remarkably clever “oxygen rebound” mechanism for cytochrome P450 hydrocarbon oxidation proposed by Groves² nearly 30 years ago is still the accepted reaction sequence (eq 1). Numerous experimental observations have been reported in support of the proposal that the reaction proceeds via a free radical oxygen rebound mechanism.^{1,2} In this consensus mechanism, it is postulated that the ferryl species ($\text{Fe}^{\text{V}}=\text{O}$) formed by cytochrome P-450-catalyzed activation of

molecular oxygen abstracts a hydrogen from the substrate to yield a one-electron reduced ferryl species ($\text{Fe}^{\text{IV}}-\text{OH}$) and a carbon radical intermediate ($\text{R}\bullet$) that recombines in the so-called oxygen rebound step² with the formal equivalent of an iron-bound hydroxyl radical, $\text{Fe}^{\text{IV}}-\text{OH}$, to give an enzyme–product complex, the final alcohol product (eq 1).^{1c,d}



However, recent developments suggest that the mechanism of substrate oxidation is far more complex than was initially believed. Mutant studies have demonstrated the existence of multiple oxidized iron species, which are capable of performing the oxidations characteristic of P450.³ Additionally, Newcomb

- (1) Ortiz de Montellano, P. R. *Cytochrome P450: Structure, Mechanism and Biochemistry*, 2nd ed.; Plenum: New York, 1995. In particular, the following chapters: (a) Groves, J. T.; Han, Y.-Z. *Cytochrome P450: Structure, Mechanism and Biochemistry*, 2nd ed.; Plenum: New York, 1995; Chapter 1, pp 3–48. (b) Mueller, E. J.; Loida, P. J.; Sligar, S. G. *Cytochrome P450: Structure, Mechanism and Biochemistry*, 2nd ed.; Plenum: New York, 1995; Chapter 3, pp 83–124. (c) Ortiz de Montellano, P. R. *Cytochrome P450: Structure, Mechanism and Biochemistry*, 2nd ed.; Plenum: New York, 1995; Chapter 8, pp 245–304. (d) Ortiz de Montellano, P. R.; DeVoss, J. J. *Nat. Prod. Rep.* **2002**, *19*, 477. (e) Hlavica, P. *Eur. J. Biochem.* **2004**, *271*, 4335.
- (2) (a) Groves, J. T.; McClusky, G. A. *J. Am. Chem. Soc.* **1976**, *98*, 859. (b) Groves, J. T.; McClusky, G. A.; White, R. E.; Coon, M. J. *Biochem. Biophys. Res. Commun.* **1978**, *81*, 154.

and his collaborators have proposed a two-oxidant model⁴ supported by radical clock studies, suggesting that a mechanism involving a long-lived substrate radical is less likely than one with competing nonsynchronous concerted and cationic pathways. However, a recent rebuttal by Groves appears to reaffirm his original position, providing very strong evidence for the existence of a long-lived carbon radical under typical reaction conditions.⁵ Everyone seems to agree on the “oxygen rebound” mechanism^{1,2} up to the point where the O₂-derived, heme iron bound hydroperoxide FeO–OH species (Cpd 0) is produced. Diverging opinions start where the distal oxygen of FeO–OH is presumably protonated (eq 1) and then a water molecule spontaneously departs to produce what is considered by most to be the primary oxidant Cpd I, an iron-oxo ferryl (formally Fe^V=O) species. The first problem is that, unlike other enzymes, there is no strategically positioned acid–base catalyst to provide the second proton to the distal oxygen of Cpd 0, such as Histidine in peroxidases, which is an obvious choice as the catalytic residue. Instead, it has been necessary to postulate rather complicated proton delivery mechanisms for which only indirect evidence is available. With P450_{cam}, it has been necessary to postulate a water molecule in the oxy complex that serves as the proton donor. This problem remains unresolved to date, and recent extensive QM/MM studies have pointed out serious problems with this proton relay theory, adding to the controversy.¹⁶

Many of the detailed experimental studies of monooxygenases have focused on the bacterial P450_{cam} (for which camphor is the substrate), the first soluble P450 protein to have its sequence and X-ray structure determined.^{7,8} The complex pathway from the inactive resting species to the putative catalytically active ferryl-oxene species (often referred to as compound I) is believed to be common across different P450 members and involves sequential changes in oxidation state, ligand composition, and spin state of the heme.^{9–11} In the substrate binding and displacement of a loosely bound water ligand, one-electron reduction of the iron occurs, after which molecular oxygen binds,

forming the last quasi-stable P450 intermediate.¹² Subsequent formation of the supposed catalytically active compound I requires a second reduction and the addition of two protons.¹³ There is substantial *indirect evidence*¹⁴ that the hydroxylation mechanism proceeds via abstraction of a hydrogen from the camphor substrate. However, there is little direct experimental data concerning the ferric superoxide reduction and protonation steps in eq 1. These questionable aspects of the catalytic cycle were the principal focus of our initial efforts. We now suggest a new potential pathway for what transpires in the so-called black box in the oxidation sequence.

2. Results and Discussion

(a) The Origin of Low O–O Bond Dissociation Energies (BDEs). A fundamental question pertaining to the mechanism of P450 oxidation is whether the O–O bond is cleaved prior to or in concert with oxygen atom transfer to the substrate. We have recently described a new class of hydroperoxide where, in certain cases, homolytic O–O bond cleavage is attended by a unique stabilization of the resulting oxyradical fragment. This type of an elongated O–O σ bond, existing formally in an excited state, is not entirely unexpected because the simplest cyclic peroxide, dioxirane, has several higher lying singlet minima where the O–O bond is elongated above that in its ground state. GS dioxirane and its low-lying 2π , 3π , and 4π excited states¹⁵ are all discrete singlet minima with different O–O bond distances (1.53, 2.35, 2.14, and 2.20 Å)^{16a} and relative energies.^{16b}

The O–O bond in peroxyoxynitrous acid (HO–ONO) is another example of an atypical σ -bond, which exhibits a low O–O bond dissociation energy (G2, 22.0 kcal/mol).^{17,18} We have recently identified both *cis*- and *trans*-isomers of metastable singlet forms of peroxyoxynitrous acid (HO–ONO*) that have O–O bonds of 2.17 and 2.13 and are only 14.4 and 12.8 kcal/mol higher in energy than ground-state (GS) HO–ONO.¹⁸ The activation barrier for forming this metastable isomer is 14.8 kcal/mol (TS_{trans}-1, Figure 1) relative to GS peroxyoxynitrous acid ($r_{O-O} = 1.45$). During the O–O bond elongation process, the electron of the developing ONO radical fragment shifts from

- (3) (a) Coon, M. J.; Vaz, A. D. N.; McGinnity, D. F.; Peng, H. M. *Drug Metab. Dispos.* **1998**, *26*, 1190. (b) Vaz, A. D. N.; McGinnity, D. F.; Coon, M. J. *Proc. Natl. Acad. Sci. U.S.A.* **1998**, *95*, 3555. (c) Toy, P. H.; Newcomb, M.; Coon, M. J.; Vaz, A. D. N. *J. Am. Chem. Soc.* **1998**, *120*, 9718. (d) Vaz, A. D. N.; Pernecky, S. J.; Raner, G. M.; Coon, M. J. *Proc. Natl. Acad. Sci. U.S.A.* **1996**, *93*, 4644. (e) Toy, P. H.; Dhanabalasingam, B.; Newcomb, M.; Hanna, I. H.; Hollenberg, P. F. *J. Org. Chem.* **1997**, *62*, 9114. (f) Pratt, J. M.; Ridd, T. I.; King, L. J. *J. Chem. Soc., Chem. Commun.* **1995**, 2297.
- (4) (a) Newcomb, M.; Toy, P. H. *Acc. Chem. Res.* **2000**, *33*, 449. (b) Newcomb, M.; Shen, R.; Choi, S.-Y.; Toy, P. T.; Hollenberg, P. F.; Vaz, A. D. N.; Coon, M. J. *J. Am. Chem. Soc.* **2000**, *122*, 2677. (c) Toy, P. H.; Newcomb, M.; Hollenberg, P. F. *J. Am. Chem. Soc.* **1998**, *120*, 7719. (d) Chandrasena, R. E. P.; Vatsis, K. P.; Coon, M. J.; Hollenberg, P. F.; Newcomb, M. J. *Am. Chem. Soc.* **2004**, *126*, 115 and references therein. (e) Atkinson, J. K. *Biochemistry* **1994**, *33*, 10630. (f) Atkinson, J. K. *Biochemistry* **1993**, *32*, 9209.
- (5) Auclair, K.; Hu, Z.; Little, D. M.; Ortiz de Montellano, P. R.; Groves, J. T. *J. Am. Chem. Soc.* **2002**, *124*, 6020.
- (6) For an excellent discussion of the problem of the proton relay and the repeated failures to find a solution to this dilemma, see: Guallar, V.; Friesner, R. A. *J. Am. Chem. Soc.* **2004**, *126*, 8501.
- (7) (a) Poulos, T. L.; Finzel, B. C.; Howard, A. J. *J. Mol. Biol.* **1987**, *195*, 687. (b) Raag, R.; Martins, S. A.; Sligar, S. G.; Poulos, T. L. *Biochemistry* **1991**, *30*, 11420. (c) Nagano, S.; Poulos, T. L. *J. Biol. Chem.* **2005**, *280*, 31659.
- (8) (a) Schlichting, I.; Berendzen, J.; Chu, K.; Stock, A. M.; Maves, S. A.; Benson, D. E.; Sweet, B. M.; Ringe, D.; Petsko, G. A.; Sligar, S. G. *Science* **2000**, *287*, 1615. (b) Meilleur, F.; Dauvergne, M.-T.; Schlichting, I.; Myles, D. A. *Acta Crystallogr.* **2005**, *D61*, 539.
- (9) (a) Loew, G. H.; Harris, D. L. *Chem. Rev.* **2000**, *100*, 407. (b) Harris, D.; Loew, G. H. *Biophys. J.* **1994**, *66*, A137. (c) Yoshizawa, K.; Kamachi, T.; Shiota, Y. *J. Am. Chem. Soc.* **2001**, *123*, 9806. (d) Kamachi, T.; Yoshizawa, K. *J. Am. Chem. Soc.* **2003**, *125*, 4652.
- (10) (a) Shaik, S.; Kumar, D.; de Visser, S. P.; Altun, A.; Thiel, W. *Chem. Rev.* **2005**, *105*, 2279. (b) Meunier, B.; de Visser, S. P.; Shaik, S. *Chem. Rev.* **2004**, *104*, 3947. (c) de Visser, S. P.; Ogliaro, F.; Harris, N.; Shaik, S. *J. Am. Chem. Soc.* **2001**, *123*, 3037. (d) Ogliaro, F.; De Visser, S. P.; Shaik, S. *J. Inorg. Biochem.* **2001**, *86*, 363. (e) Ogliaro, F.; Harris, N.; Cohen, S.; Filatov, M.; de Visser, S. P.; Shaik, S. *J. Am. Chem. Soc.* **2000**, *122*, 8977. (f) Kumar, D.; de Visser, S. P.; Shaik, S. *J. Am. Chem. Soc.* **2005**, *127*, 8204. (g) Sharma, P. K.; Kevorkiants, R.; de Visser, S. P.; Kumar, D.; Shaik, S. *Angew. Chem., Int. Ed.* **2004**, *43*, 1129.
- (11) (a) Guallar, V.; Gherman, B. F.; Miller, W. H.; Lippard, S. J.; Friesner, R. A. *J. Am. Chem. Soc.* **2002**, *124*, 3377. (b) Davydov, R.; Macdonald, I. D. G.; Makris, T. M.; Sligar, S. G.; Hoffman, B. M. *J. Am. Chem. Soc.* **1999**, *121*, 10654.
- (12) (a) Egawa, T.; Ogura, T.; Makino, R.; Ishimura, Y.; Kitagawa, T. *J. Biol. Chem.* **1991**, *266*, 10246. (b) Bangcharoenpaupong, O.; Rizzo, A. K.; Champion, P. M.; Jollie, D.; Sligar, S. G. *J. Biol. Chem.* **1986**, *261*, 8089.
- (13) Aikens, J.; Sligar, S. G. *J. Am. Chem. Soc.* **1994**, *116*, 1143.
- (14) Davydov, R.; Makris, T. M.; Kofman, V.; Werst, D. E.; Sligar, S. G.; Hoffman, B. M. *J. Am. Chem. Soc.* **2001**, *123*, 1403.
- (15) (a) Wadt, W. R.; Goddard, W. A., III. *J. Am. Chem. Soc.* **1975**, *97*, 3004. (b) Harding, L. B.; Goodard, W. A., III. *J. Am. Chem. Soc.* **1978**, *100*, 7180.
- (16) (a) Bach, R. D.; Owensby, A. L.; Andres, J. L.; Schlegel, H. B. *J. Am. Chem. Soc.* **1991**, *113*, 7031. (b) Bach, R. D.; Andrés, J. L.; Owensby, A. L.; Schlegel, H. B.; McDouall, J. J. W. *J. Am. Chem. Soc.* **1992**, *114*, 7207. (c) Bach, R. D.; Ayala, P. Y.; Schlegel, H. B. *J. Am. Chem. Soc.* **1996**, *118*, 12758.
- (18) (a) Bach, R. D.; Dmitrenko, O.; Estevez, C. M. *J. Am. Chem. Soc.* **2003**, *125*, 16204. (b) Bach, R. D.; Dmitrenko, O.; Estevez, C. M. *J. Am. Chem. Soc.* **2005**, *127*, 3140.

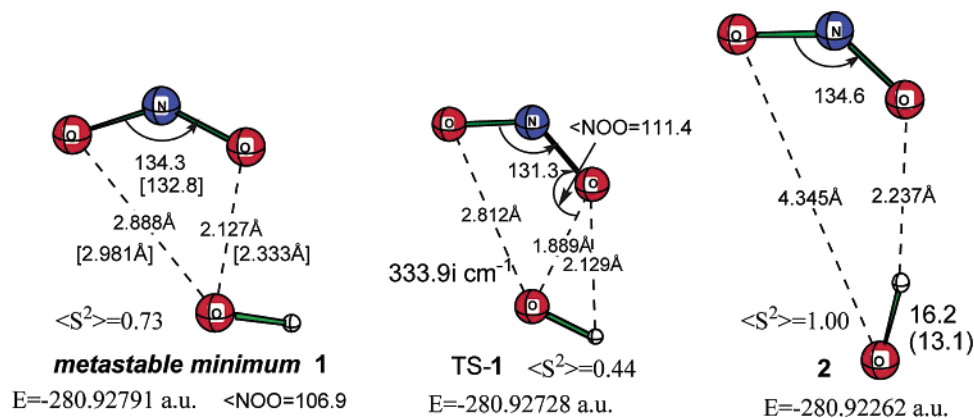


Figure 1. UB3LYP/6-311+G(3df,2p)-optimized biradicaloid minima for the metastable singlet form of peroxyxynitrous acid **1**, its transition structure (TS-1) for formation from the trans-conformer of ground-state HO–ONO, and isomer **2**, the $2A^1$ ground-state ONO radical weakly hydrogen bonded to OH radical. Geometrical data in brackets are at the CAS(12,10)/6-311+G(d,p) level.

being localized largely on the oxygen of the O–O bond to the central nitrogen atom of the ONO fragment, thereby relaxing to the lower energy 2A_1 ground-state ONO radical and recovering a part of the potential energy (30.2 kcal/mol)^{18b} associated with this 2B_2 to 2A_1 electronic transition. It is this electronic reorganization attending O–O bond elongation that is responsible for the stabilization of the singlet metastable state of peroxyxynitrous acid (HO \cdots ONO*).

A weakly hydrogen-bonded form, **2**, of this metastable isomer exists as a minimum that is 16.2 kcal/mol higher in energy than GS HO–ONO. Thus, peroxyxynitrous acid represents an exceptional type of peroxide where O–O bond cleavage is attended by a unique stabilization of one of the resultant oxy radical fragments. Both alkyloxyl (RCO $_2$)¹⁷ and NO $_2$ radicals¹⁹ have a σ ground state, but both also have σ and π types of orbitals. For peracids, the electron spin is delocalized up in the π system, and, in contrast, this does not provide an opportunity for any special type of stabilization and hence peracids have rather typical O–O BDEs ($47\text{--}48 \text{ kcal/mol}$).¹⁷

Another type of peroxide bond where an exceptional opportunity exists for resonance stabilization of an oxyradical is where the incipient oxygen radical is conjugated to a carbon–carbon double bond. We reported earlier^{17,18b} that simple vinyl hydroperoxides (H $_2$ C=CHO–OH) such as isopropenyl hydroperoxide have an atypically low O–O BDE (20.2 kcal/mol , G3) due to the delocalization of the O-centered radical to a C-centered radical. Cleavage of the O–O bond in isopropenyl hydroperoxide produces a putative isopropenyloxy radical with the spin on oxygen oriented in the σ plane of the molecule (σ^2A') that corresponds to a more normal O–O BDE of 42.9 kcal/mol (G3). However, in this case, the electronic spin density prefers to reside on the carbon atom, resulting in a stabilization energy of 23.1 kcal/mol ($\Delta E_{\delta\pi}$, G3) due to electron delocalization in the π system. Equilibrium O–O bond dissociation correlates with the lower lying π^2A'' state, and the O–O BDE is dramatically reduced to 19.6 kcal/mol (G3).

Phenyl hydroperoxide exhibits the same behavior with an O–O BDE of only 20.2 kcal/mol for exactly the same reasons.

For the sake of comparison, the O–O BDE for the isopropenyl and phenyl hydroperoxides are 13.3 and 14.9 kcal/mol at the B3LYP/6-311+G(d,p) level. Obviously, with O–O BDEs of this low magnitude, neither hydroperoxide has ever been isolated. The transition structures (Figure 2) for conversion of the GS hydroperoxides to their corresponding hydroxyl radical-hydrogen-bonded minima at the UB3LYP/6-311+G(d,p) level of theory (TS-**3** $\langle S^2 \rangle = 0.61$ and TS-**4** $\langle S^2 \rangle = 0.77$) have $\Delta E^\ddagger = 14.3$ and 14.4 kcal/mol . The inverted hydrogen-bonded minima **3** and **4** (C=C–O \cdots HO) are only 10.5 and 11.3 kcal/mol higher in energy than their GS hydroperoxides. In this overall process, when a weak O–O bond is identified and a metastable minimum exists with an O–O bond distance $\sim 2 \text{ \AA}$, the TS for formation of this excited state typically lies very close in energy to this “excited” minimum and is connected to the hydrogen-bonded hydroxyl form. Because both **3** and **4** are neutral species, their H-bonding energies are relatively small (7.0 and 7.3 kcal/mol).

The lesson to be gleaned from this discourse is that O–O bond dissociation attended by some form of unique stabilization of the oxyradical produced can be directly responsible for an exceptional type of peroxy bond that can undergo this type of somersault or vault motion to a stabilized hydroxyl radical intermediate. The myriad of electronic states associated with metal-based hydroperoxides presents another unique opportunity to observe this new class of transient hydroperoxide. We anticipated and found that just such an extraordinary reduction in bond dissociation energy (BDE = 22.9 kcal/mol) accompanies homolytic O–O bond cleavage in a porphyrin iron(III) hydroperoxide (FeO–OH)!

(b) The Somersault Step for Porphyrin Iron(III) Hydroperoxide Rearrangement. For a number of years, we have augmented our mechanistic studies by first determining accurately (G2 and G3) a series of O–O bond dissociation energies to guide us energetically.²⁰ The heme systems are much larger, and we must be content with BDE determined at a somewhat lower level [6-311+G(d,p)] but calibrated, when possible, with the G2 or G3 level. The O–O BDEs vary considerably when a smaller basis set (6-31G) is used for oxygen. For example, the OH anion is more

(19) (a) Davidson, E. R. *J. Am. Chem. Soc.* **1977**, *99*, 397. (b) For recent studies on potential energy surfaces of NO $_2$, see: (b) Kurkal, V.; Fleurat-Lessard, P.; Schinke, R. *J. Chem. Phys.* **2003**, *119*, 1489. (c) Mahapatra, S.; Köppel, H.; Cederbaum, L. S.; Stampfuss, P.; Wenzel, W. *Chem. Phys.* **2000**, *259*, 211.

(20) (a) Bach, R. D.; Dmitrenko, O. *J. Org. Chem.* **2002**, *67*, 2588. (b) Bach, R. D.; Dmitrenko, O. *J. Am. Chem. Soc.* **2004**, *126*, 4444.

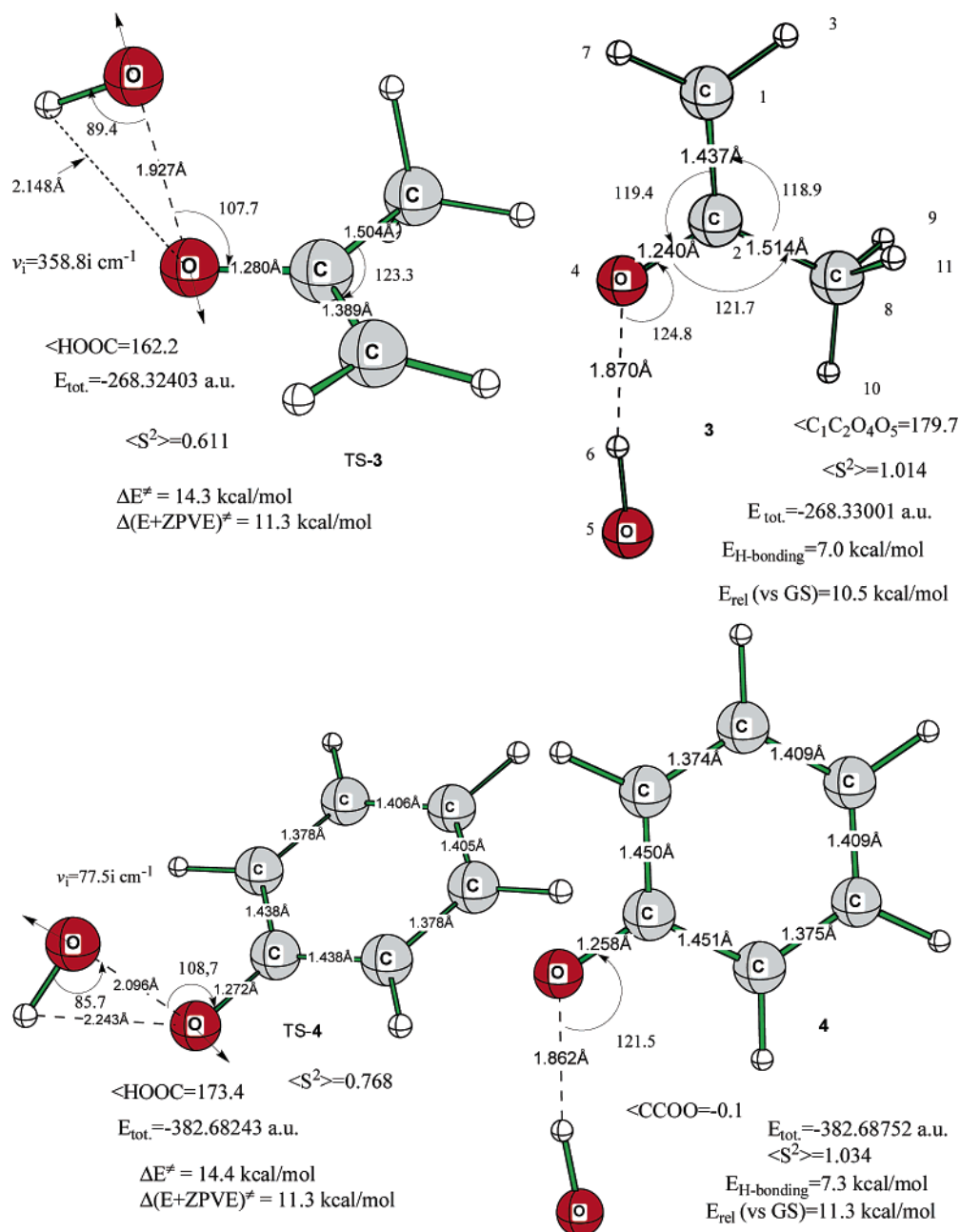


Figure 2. UB3LYP/6-311+G(d,p)-optimized transition structures connected to their ground-state hydroperoxides on the reactant side and biradicaloid hydrogen-bonded product minima on the product side for isopropenyl hydroperoxide (TS-3 and 3) and phenyl hydroperoxide (TS-4 and 4) –OOH group isomerizations.

stable than the OH radical by 1.1 kcal/mol with the 6-31G basis but 34.0 kcal/mol with the larger basis [6-311+G(d,p)]. At the G3 level, this energy difference is 41 kcal/mol. In the present case, this somersault rearrangement should only take place with a relatively weak O–O bond. The O–O BDE for the simplest porphyrin FeO–OH doublet (**5**, Figure 3) is only 22.9 kcal/mol; we anticipated that such a low BDE would be associated with the existence of a hydrogen-bonded hydroxyl radical excited state (Fe=O···HO*). Homolytic O–O bond cleavage in **5** correlates with the neutral triplet $^3A_g(\text{Fe}^{\text{IV}})$ “oxyradical” fragment that is 11.6 kcal/mol lower in energy than the corresponding $^5\Delta(\text{Fe}^{\text{IV}})$ quintet state.²¹ By comparison, the O–O BDE for H_2O_2 is 44.1 kcal/mol at this level [B3LYP/6-311+G(d,p)] and 50.45

kcal/mol at the G2 level.¹⁷ The structure of the energy minimum for GS iron(III) hydroperoxide **5** proved to be very close to that previously reported by Shaik (see Computational Details).¹⁰

Prior experience with peroxyxynitrous acid¹⁸ taught us that we needed a relatively flexible basis set for oxygen [6-311+G(d,p)] that contains both a plus basis (for the oxygen lone-pairs) and polarization functions on hydrogen to be able to locate these H-bonded transient hydroperoxide excited states.¹⁸ The doublet configuration of ground-state (GS) hydroperoxide **5** was found to be 0.6 kcal/mol more stable than the quartet and much more

(21) For a comprehensive study of the relative energies of these intermediate states, see: Ogliaro, F.; de Visser, S. P.; Cohen, S.; Sharma, P. K.; Shaik, S. *J. Am. Chem. Soc.* **2002**, *124*, 2806.

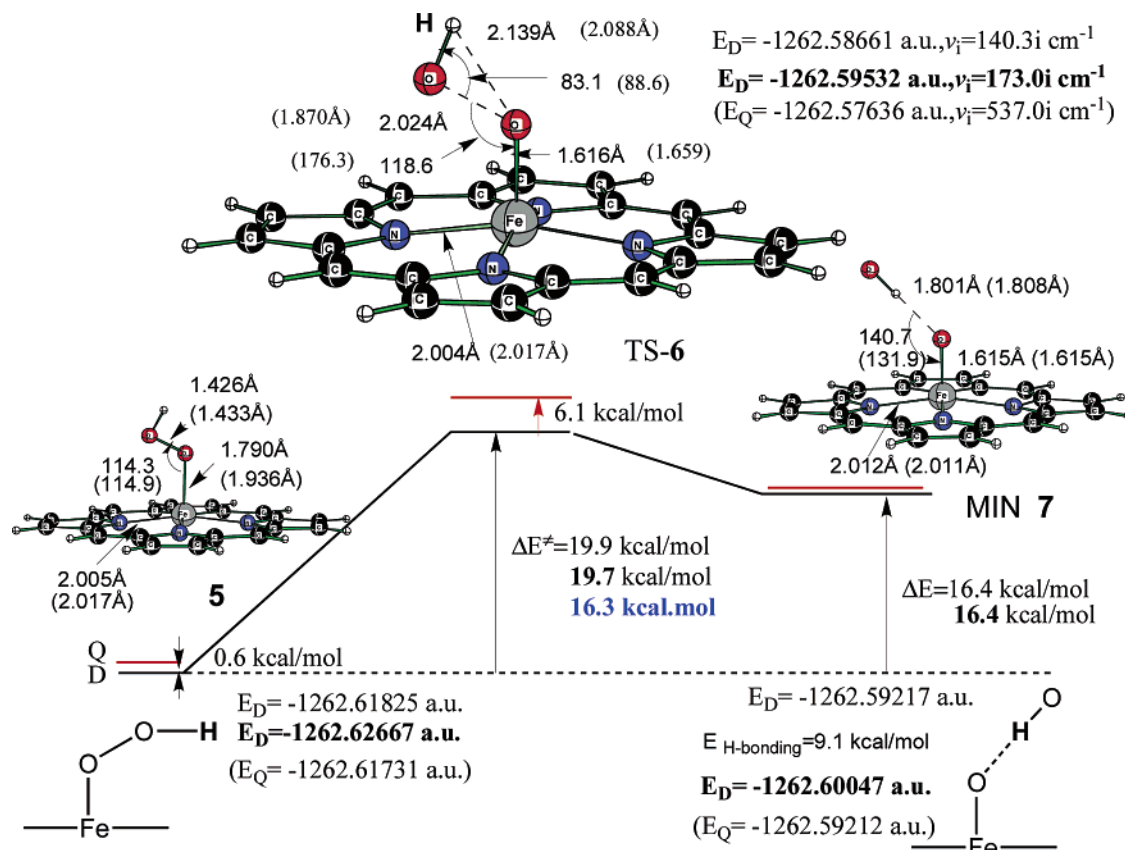


Figure 3. Somersault reaction energy diagram (letters “D” and “Q” refer to doublet and quartet states). Energy levels of quartet GS porphFeOOH (5) and H-bonded porphFeO...HO (MIN 7) structures are remarkably close to the corresponding doublets and are represented by red lines. The energies and geometries in parentheses are from optimized quartet structures. Numbers in plain are calculated with the 6-311+G(d,p) basis set on the oxygen atoms (308 basis functions and 705 primitive Gaussians). Numbers in bold are calculated with the 6-311+G(d,p) basis set on oxygens and hydrogen of the OOH group (314 basis functions and 713 primitive Gaussians). The ΔE^\ddagger in blue has the 6-311+G(d,p) basis set on the Fe atom, the four N atoms, in addition to the OOH moiety.

stable than a sextet (Table S3, Supporting Information). The Fe–O and O–O bond distances in the GS were 1.79 and 1.426 Å. The rearrangement of the FeO–OH moiety basically just involves O–O bond elongation. Animation of the single imaginary frequency for TS-6 (Figure 3) shows largely O–O bond elongation with a pendulum motion of the oxygen of the OH group and very little movement of the OH hydrogen atom. Although we cannot yet do an IRC calculation, it appears as though TS-6 is connected to GS-5 FeO–OH on the reactant side and a minimum with an elongated O–O bond much in the same way as the HO–ONO metastable form above (Figure 1). We have located what is most likely this minimum (not shown) that has a total energy essentially identical to that of the TS but has two very small imaginary frequencies (11.0i cm^{-1}). It is not uncommon for an endothermic process to have the TS and resulting minima on the product side very close in energy and difficult to locate. The activation energy for the FeO–OH rearrangement process is 19.9 kcal/mol, and the H-bonded minimum resulting from this “somersault” activity is only 16.4 kcal/mol above the GS FeO–OH (Figure 3). The transition state for this rearrangement has an O–O distance of 2.02 Å and bears a close resemblance to the TS for the corresponding HO–ONO rearrangement (Figure 1).¹⁸ The resulting isomeric hydroperoxide 7, with an hydroxyl radical hydrogen bonded to the ferryl oxygen, is only 3.5 kcal/mol lower in energy than TS-6. The porphyrin ring in 5 acts as an electron donor, and we see a decrease in electron density in the porphyrin ring of 0.15 e at

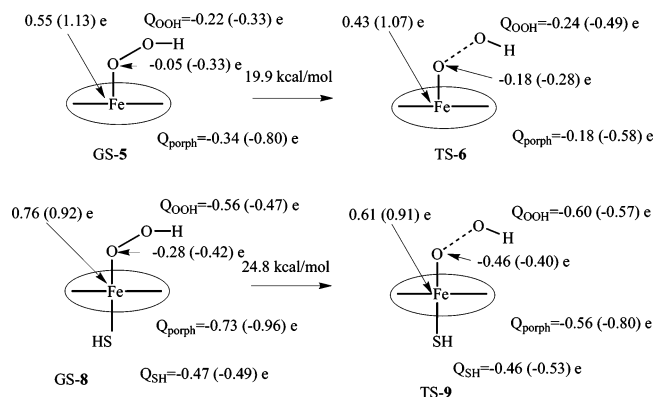


Figure 4. APT and NBO (in parentheses) charge distributions in the PorFeOOH (neutral) and Por(SH)FeOOH (anionic) ground-state minima and their corresponding transition structures for the FeO–OH isomerization.

the TS for formation of isomeric MIN-7 (FeO...HO). A summary of changes in the charge distribution upon going from GS to TS-6 is given in Figure 4.

The primary change is an increase in electron density on the Fe itself (0.12 e) that is supplied largely by the porphyrin ring. Although the net electron density of the OOH moiety does not change much, the electron density of the incipient ferryl oxygen increases, making it more basic in the TS as the O–O bond is cleaved during the somersault motion of the hydroperoxide. Homolytic O–O bond cleavage in GS-5 correlates with the

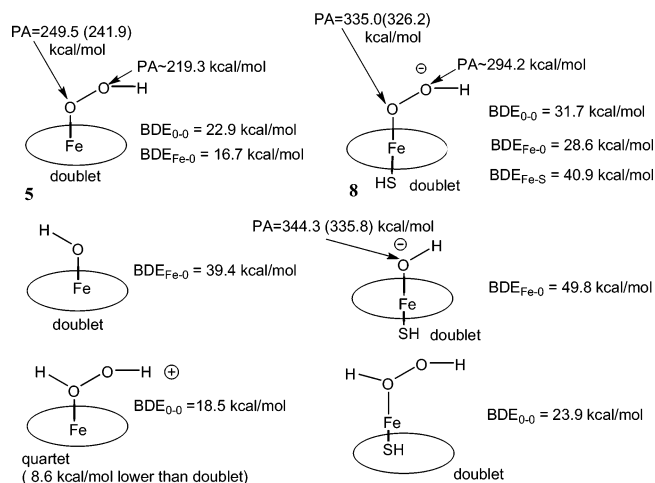


Figure 5. Calculated proton affinities (PA) and bond dissociation energies (BDE) in **5** and **8**. PAs are based upon total energies; numbers in parentheses are with ZPVE corrections. BDEs are based upon enthalpies. The “~” sign indicates a value estimated by freezing the O–O bond distance to that in its parent hydroperoxide.

triplet $^3A_g(\text{Fe}^{\text{IV}})$ state of the $\text{Fe}=\text{O}$ heme that is 11.6 kcal/mol lower in energy (Table S2b, Supporting Information) than its corresponding quintet $^5\Delta(\text{Fe}^{\text{IV}})$ state, providing additional stabilization of the “oxyradical” fragment and contributing to the relatively low O–O BDE in GS-**5**. The activation barrier for this unusual metal hydroperoxide isomerization ($\text{FeO}-\text{OH} \rightarrow \text{FeO}\cdots\text{HO}$) is reduced to 16.3 kcal/mol (Figure 3) when the basis set balance is improved by including the 6-311+G(d,p) basis set on Fe, N, and OOH. We have also supported this unusual DFT-optimized TS-**6** by CASSCF calculations. Using a (9,9) active space, consisting of oxygen lone pairs and Fe d-orbital combinations, we located a first-order saddle point for the OOH rearrangement. This optimized TS (quartet) has geometrical parameters consistent with those for DFT-optimized TS-**6** ($r_{\text{O}-\text{O}} = 1.97 \text{ \AA}$, $r_{\text{Fe}-\text{O}} = 1.75 \text{ \AA}$, $\angle_{\text{FeOO}} = 84.2^\circ$). The orbital occupations were 1.94, 1.72, 1.94, 1.04, 1.04, and 0.97 and 0.31, 0.02, and 0.02 electrons. This TS exhibits some quintet character due to a 0.35 electron excitation into the virtual space.

Rearrangement of the $\text{FeO}-\text{OH}$ group in the absence of the Cys^{357} anion (SH^-) suggests the possibility that such activity of a metal hydroperoxide may prove to be quite general for those cases where the resulting $\text{M}=\text{O}$ fragment enjoys a special type of stabilizing influence that simply derives from a lower lying electronic state. It is particularly noteworthy that the activation barrier for the somersault is lower without the coordination of a thiolate ligand. When the HS^- is present, the activation barrier for the rearrangement step increased by 4.9 kcal/mol for the doublet state. This is perhaps not too surprising because the O–O BDE (Figure 5) increases from 22.9 kcal/mol in hydroperoxide **5** to 31.7 kcal/mol when the HS^- ligand is present in anionic hydroperoxide **8** (Figure 6). This appears to be counterintuitive because it has long been assumed that one of the functions of the Cys^{357} residue is to increase the electron density in the system, thereby effecting a *weakening* of the O–O bond.

The quartet state for this anionic OOH rearrangement TS (Figure 6) has so far presented problems, but our best estimate is that it will be somewhat higher in energy. This may well be due to the higher energy of the quartet state of **8**. To validate

this point, we used a more balanced basis set on the critical atoms that included the 6-311+G(d,p) basis set on Fe, SH, N, and OOH. We found upon full geometry optimization that the doublet state of ground-state $\text{FeO}-\text{OH}$ **8** was 13.0 kcal/mol more stable than the quartet state. This again provides justification for examining this PES with the doublet state. The O–O bond distance in TS-**9** is essentially the same as that in TS-**6** (without the HS^- present), and the Fe–O distance is only slightly longer. The Fe–S distance in TS-**9** (2.487 Å) is about what is expected based upon numerous X-ray studies.^{7,8} MIN-**10** is formally Cpd II, the one-electron reduced form of Cpd I, hydrogen-bonded to an $\text{HO}\bullet$ radical. The $\text{HO}\bullet$ radical is H-bonded in nearly a linear inverted fashion to the ferryl oxygen of the heme with a relatively short $\text{O}\cdots\text{HO}$ distance of 1.66 Å, reflecting the anionic nature of the donor.

As noted above, when the larger basis set [6-311+G(d,p)] is also included on the hydrogen of the OOH group, the classical activation barrier for $\text{FeO}-\text{OH}$ isomerization, TS-**9**, is slightly reduced ($\Delta E^\ddagger = 24.3 \text{ kcal/mol}$). When the larger basis set is also included on the Fe atom, this barrier is reduced to 20.3 kcal/mol, presumably reflecting the better basis set balance (Figure 6). Significantly, this H-bonded hydroxyl radical MIN-**10** is only 17.5 kcal/mol higher in energy than GS **8**. Because the O–O bond dissociation energy (BDE = 31.7 kcal/mol) is well above the relative energy of MIN-**10** (Figure 6), the OH radical is bound by $\sim 14 \text{ kcal/mol}$.

A related hydroxyl radical bound species has been invoked in the mechanism of heme degradation by the enzyme heme oxygenase (HO). Shaik and co-workers have suggested that *meso*-hydroxylation of the heme in HO utilized an $\text{FeO}\cdots\text{HO}$ intermediate comparable to MIN-**10** but with an imidazole axial ligand instead of a thiolate.^{10f,g}

The orientation of the hydroxyl radical in MIN-**10**, with respect to the ferryl oxygen, is to be expected because recent high level calculations²¹ show the hydrogen-bonding topology for the minimum-energy structure of hydrated hydroxyl radical to be of C_s symmetry where the $\text{H}-\text{O}\bullet$ acts as a proton donor with the unpaired electron in the reflection plane of the water molecule ($2A'$ state). The computed well depth for this $\text{OH}-\text{OH}_2$ complex is about 5.6 kcal/mol (Figure 7)^{22b} as compared to 9.1 kcal/mol in neutral MIN-**7** and 17.0 kcal/mol in negatively charged MIN-**10**.

If the activation barrier for the model “ $\text{FeO}-\text{OH}$ somersault” is increased in the presence of the SH^- , what then is the role of the Cys^{357} in the enzymatic oxidation? We suggest, at this point, that at least one purpose of the cysteine anion is to increase the stability of the hydrogen bond of metastable hydroxyl radical MIN-**10**. In the present case, it is particularly important to establish that these intermediates are not just weakly hydrogen-bonded hydroxyl radicals; the H-bonding energy in anionic complex MIN-**10** (HS^- present) is 17 kcal/mol. The magnitude of this stabilization is relevant to the lifetime of this metastable isomeric hydroperoxide because it would appear to be sufficiently stable to survive long enough to achieve hydrogen abstraction from the hydrocarbon substrate. It is also important because a stabilization energy this large removes any speculation about the credibility of MIN-**10** as a viable minimum due to

(22) (a) Ohshima, Y.; Sato, K.; Sumiyoshi, Y.; Endo, Y. *Am. Chem. Soc.* **2005**, *127*, 1108. (b) Brauer, C. S.; Sedo, G.; Grumstrup, E. M.; Leopold, K. R. *Chem. Phys. Lett.* **2005**, *401*, 420.

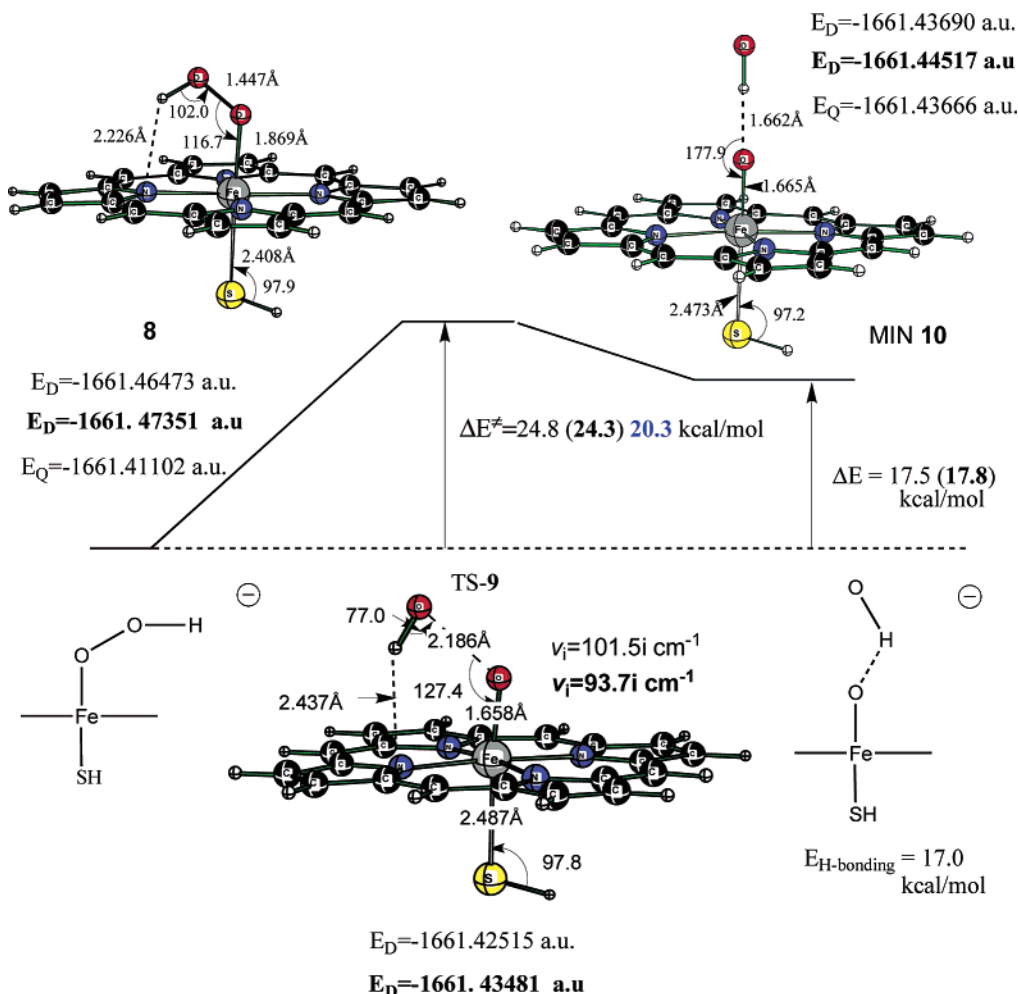


Figure 6. The B3LYP reaction energy diagram for the FeO–OH somersault rearrangement in the presence of the thiolate anion (HS[−]). Letters “D” and “Q” refer to doublet and quartet states. The total energy values for OH radical (−75.75367 au) and Por(SH)FeO triplet anion (−1585.65609 au) were taken for the H-bonding energy estimation. Numbers in plain are calculated with the 6-311+G(d,p) basis set on the O–O oxygens (323 basis functions and 755 primitive Gaussians). Numbers in bold are calculated with the 6-311+G(d,p) basis set on both oxygen and hydrogen of the OOH group (329 basis functions). The ΔE^\ddagger in blue has the 6-311+G(d,p) basis set on the Fe atom, in addition to the OOH moiety.

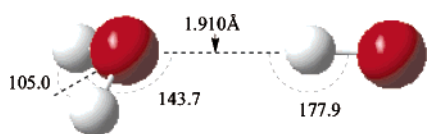


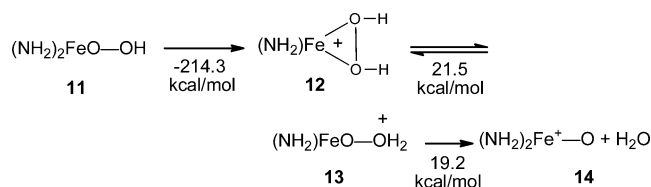
Figure 7. The orientation of the hydrogen-bonding interaction of hydroxyl radical with a water molecule (see ref 22 for details).

the potential role of basis set superposition error or ZVPE corrections being large enough to question its existence. The increased basicity of the anionic complex, especially the ferryl oxygen (Figure 4), also facilitates the isomerization step (TS-9) and in the later stages the obligatory concerted transfer of an H atom from water to the ferryl oxygen in the hydroxylation step (see below). We will examine further the role of Cys³⁵⁷ below. There is a similar increase in electron density of the Fe in TS-9 and a decrease in electron density (0.17 e) in the porphyrin ring as noted above for TS-6 (Figure 4). The anionic “oxyradical” fragment resulting from homolytic O–O bond cleavage in hydroperoxide **8** correlates with the $^3A_g(\text{Fe}^{\text{IV}})$ triplet state and is 28.3 kcal/mol lower than the singlet $^1A_g(\text{Fe}^{\text{IV}})$ state and 38.3 kcal/mol lower in energy than the $^5A_{2u}(\text{Fe}^{\text{III}})$ quintet state.²¹ The possibility of multiple lower energy states contrib-

utes to the relatively low O–O BDE and the potential for this novel somersault mechanism to readily occur with certain metal hydroperoxides. The activation energy for this isomerization is typically much lower than the O–O bond dissociation limit because the O–O–H angle is always less than 90° in the TS due to a hydrogen-bonding interaction of the hydrogen with the proximal oxygen as O–O bond cleavage ensues. In many cases, this O–O–H angle and the interaction of this hydrogen with the proximal oxygen are part of the reaction vector for OOH rearrangement.¹⁸

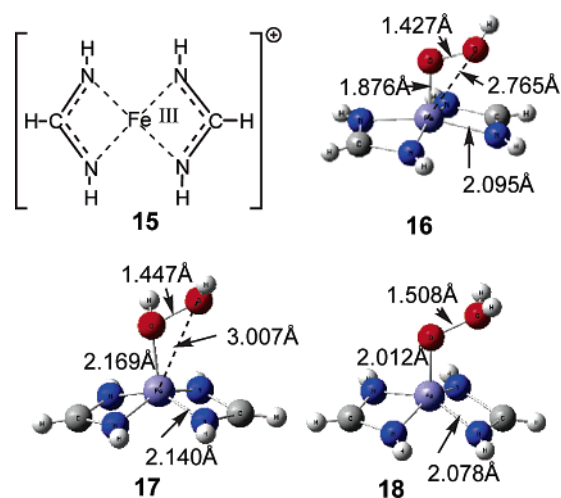
(c) Perceived Problems Associated with the Accepted “Oxygen Rebound” Mechanism. The “oxygen rebound” step in the consensus mechanism^{1,2} seems quite logical once you have arrived at the ferryl oxygen stage [Fe^V=O]. However, more than a decade ago, we questioned the first part of the reaction sequence that generates the ferryl oxygen complex (Cpd I) by two successive protonation steps. Our objections were based simply upon O–O bond energy considerations.^{23a,b} We examined the thermodynamic properties of a highly abbreviated model iron(III) hydroperoxide **11** and its protonated forms. In most of the simple iron(III) compounds considered, the sextet proved to be lower in energy as one might expect in the absence

of the perturbation of the Fe atom by the nitrogen lone pairs associated with the porphyrin. With full geometry optimization (numerically) at the Brueckner doubles (BD) level (BD/WH basis set),^{23d} the O–O bond dissociation energy for cation **12** is predicted to be only 20.7 kcal/mol ($D_e = 22.3$ kcal/mol at the MP4//MP2/WH level).^{23a} A similar all-electron calculation with an extended basis set gave thermodynamic properties in excellent agreement with experiment for a series of iron halides.²⁴



With all electron calculations and the WH basis set (47 basis functions on iron) and a DZ quality basis set (MP4//MP2/WH) for the other heavy atoms, we predicted^{23a} that the overall process for forming a ferryl oxygen species from $(\text{NH}_2)_2\text{FeO}-\text{OH}$ would be highly endothermic (40.7 kcal/mol). Because the bridged structure **12** is 21.5 kcal/mol lower in energy than that derived from protonation of the distal oxygen, **13**, a subsequent heterolytic O–O bond cleavage affording ferryl oxygen [Fe(V)=O] species **14** is questionable because a meaningful equilibrium concentration of **13** is unlikely. This is not totally unexpected because a 1,2-hydrogen shift producing the water oxide form of hydrogen peroxide, $\text{H}_2\text{O}-\text{O}$, is 50 kcal/mol^{23a} higher in energy than GS HO–OH and the barrier for the reverse reaction regenerating HO–OH is only 3.2 kcal/mol.²⁵ The barrier for a 1,2-hydrogen shift in **12** producing distal diprotonated **13** was reported to be 49.1 kcal/mol.^{23a} One should not anticipate the behavior for the hydrogen shift in **12** producing **13** to be much different from protonated hydrogen peroxide itself [HO–OH₂⁺]. To provide a comparison with the current methods given below, using the LAN2DZ ECP for iron and a 6-311+G(d,p) basis set for the other atoms, the O–O BDEs for **11**, **12**, and **13** are 32.9, 19.0, and 7.4 kcal/mol, respectively. The PA for distal protonation of FeO–OH to produce FeOOH_2^+ **13** is 185.7 kcal/mol, while the PA for the proximate oxygen is 207.0 kcal/mol (with ZPVE, $\Delta\text{PA} = 21.3$ kcal/mol). The BDEs here and elsewhere are based upon enthalpic data (ΔH_{298}).

With these preliminary data in hand, we investigated a slightly larger, but nonconjugated, porphyrin model **15** where we arrived at basically the same conclusions. In these recent calculations, we have considered only the sextet state because this appears to be the lowest energy state in most cases. Protonation of bis-imine model **16** on the proximal oxygen affords protonated iron hydroperoxide **17**.



Protonation of FeO–OH can occur on either oxygen, giving the hydrogen peroxide intermediate **17** or the *higher energy* water oxide adduct **18**. The difference in energy between **17** and **18** is 24.6 kcal/mol (Table S1 in the Supporting Information). The O–O BDEs for **16** and **17** are 37.6 and 34.1 kcal/mol [B3LYP/6-311+G(d,p), basis set on oxygen]. Compound **18** is a weakly bonded water complex with an O–O bond energy of 0.5 kcal/mol and is 24.4 kcal/mol higher in enthalpy than **17**. ZPVE correction results in an antibonding character of the O–O bond in **18**, and the water molecule is not bound.

One of our fundamental concerns when initially challenging²³ the accepted steps leading to the formation of the consensus oxidizing agent Cpd I (eq 1) is that we perceived that a simple iron(III) hydroperoxide such as **11** should exhibit basically the same thermodynamic behavior with respect to O–O bond cleavage with and without the surrounding porphyrin system. Major controversy still surrounds the requirement for spurious water molecules in a proton relay,⁶ and the source of the second proton required for protonation of the distal oxygen in FeO–OH remains in question. The proton affinity (PA) for the proximal oxygen of the neutral iron(III) porphyrin hydroperoxide **5** is 249.5 kcal/mol, while that of the distal oxygen is estimated to be 219.3 kcal/mol (Figure 5). The $\Delta\text{PA} = 30.2$ kcal/mol for the proximal versus distal oxygen atoms of this porphyrin iron hydroperoxide **5** is slightly larger than that noted above for the simpler d⁵-iron hydroperoxides. However, when the distal oxygen in **5** is protonated to produce the cationic water oxide form [FeO–OH₂⁺], the O–O bond breaks simultaneously to produce a water molecule and the porphyrin Fe–O cation, a situation not that different from that noted for the formation of **13**. These data, however, pertain to potential intermediates prior to ligation by Cys³⁵⁷(HS[−]).

Addition of HS[−] to the iron center in FeO–OH **5** produces anionic complex **8** that possesses a *stronger* O–O bond (BDE = 31.7 kcal/mol). We also see a greater BDE for the Fe–O bond in both the hydroperoxide and the hydroxide [Fe–OH] when the thiolate is included. The Fe–S BDE is 40.9 kcal/mol; however, a heterolytic cleavage with the loss of HS[−] is energetically favored ($\Delta H^\circ = 33.7$ kcal/mol) as noted earlier by Shaik.²¹ The O–O BDE (23.9 kcal/mol) of the proximally protonated heme hydroperoxide **8** is also increased, and it is noteworthy that the O–O BDE for this model porphyrin system is approximately the average of the simple iron(III) hydrogen peroxide adducts **12** and **17** shown above. The most significant

- (23) (a) Bach, R. D.; Su, M.-D.; Andres, J. L.; Schlegel, H. B. *J. Am. Chem. Soc.* **1993**, *115*, 8763. (b) Bach, R. D.; Mintcheva, I.; Estvez, C. M.; Schlegel, H. B. *J. Am. Chem. Soc.* **1995**, *117*, 10121. (c) Bach, R. D.; Schlegel, H. B.; Andres, J. L. *J. Am. Chem. Soc.* **1994**, *116*, 3475. (d) Bach, R. D.; Andres, J. L.; Su, M.-D.; McDouall, J. J. W. *J. Am. Chem. Soc.* **1993**, *115*, 5768. (e) Bach, R. D.; Su, M.-D. *J. Am. Chem. Soc.* **1994**, *116*, 10103. (f) Canepa, C.; Bach, R. D.; Dmitrenko, O. *J. Org. Chem.* **2002**, *67*, 8653.
- (24) (a) Bach, R. D.; Shobe, D. S.; Schlegel, H. B.; Nagel, C. J. *J. Phys. Chem.* **1996**, *100*, 8770. (b) Glukhovtsev, M. N.; Bach, R. D.; Nagel, C. J. *J. Phys. Chem. A* **1997**, *101*, 316.
- (25) Huang, H. H.; Xie, Y.; Schaefer, H. F., III. *J. Phys. Chem.* **1996**, *100*, 6076.

point to be made in this comparison is that there is even a greater estimated difference in the proton affinities of the two oxygens of the FeO–OH group in anionic hydroperoxide **8**. Estimates of the PA of the two oxygens in **8** (with the O–O bond frozen at 1.45 Å) suggest an *energy penalty* of about 40 kcal/mol for protonation of the distal relative to the proximal oxygen.⁶ It is therefore questionable whether a proton source approaching the FeO–OH region at the active site would protonate the distal rather than the proximal oxygen. In a recent QM/MM study, Friesner⁶ stated that “a second protonation (on the distal oxygen) from replaced Thr252 requires an energy greater than 14 kcal/mol (constraining the O–H to 1.05 Å) and a stable structure did not result”. It is also unlikely that a 1,2-hydrogen shift from the proximal to the distal oxygen could accomplish this because this is also associated with a high barrier.^{23b} Shaik²¹ has reported an estimated PA for the distal oxygen of MIN-10 of –330 kcal/mol and also reported a spontaneous O–O bond breaking with the loss of water to produce Cpd I. The same barrierless loss of water upon protonation of the distal oxygen of MIN-10 was reported earlier by Harris and Loew.²⁶ In both cases, protonation of the distal oxygen of the FeO–OH moiety was the *assumed pathway*. However, in a recent related theoretical study of the enzymatic HO• radical transfer to the *meso*-carbon of the heme in the enzyme heme oxygenase (HO), Shaik^{10f,g} reported a proton relay sequence where “free optimization of the H₃O⁺–(H₂O)₂ system resulted always in the initial protonation of the proximal oxygen of the FeOO moiety.” This regiospecific protonation was justified on the basis of structural data, suggesting the absence of a specific acid close enough to the FeO–OH moiety to partake directly in a protonation reaction, but the existence of a hydrogen-bonding network that connects to the distal side of the heme. A mechanism was proposed where the proton is relayed regiospecifically, via a structured water chain, to the proximal oxygen of FeO–OH species while the O–O bond is undergoing homolysis. However, it has always been assumed that initial protonation of the proximal oxygen would simply result in “uncoupling” producing HO–OH instead of the hydroxylation.^{7b} This would appear to be especially true because we note above that a [1,2]-hydrogen shift to produce the water oxide form of FeO–OH₂⁺ as in **13** would have a prohibitively high activation barrier. Even if you were able to protonate the distal oxygen, a [1,2]-H shift back to the proximal oxygen should be almost barrierless.^{23a,25} The question remains, can you protonate the energetically unfavorable oxygen even if the addition of a proton results in the loss of water without a barrier? It does not appear that this particular point has been adequately addressed in the myriad of prior studies on this oxidation scheme. It has even been suggested that the proton relay may only be able to reach the distal oxygen (but not the proximal), but even in this case a [1,2]-hydrogen shift back to the proximal oxygen could possibly take place before the onset of O–O bond cleavage producing a water molecule. This still remains one of the most egregious steps⁶ in the overall consensus mechanism (eq 1). Fortunately, the reaction scheme proposed in Figure 8 obviates the need for this proton delivery scheme because the relatively weak O–O bond in **8** (Cpd 0) can homolytically cleave upon FeO–OH isomerization to afford primary oxidant MIN-10 with a relatively low (gas phase) activation barrier ($\Delta E^\ddagger = 20.3$ kcal/mol).

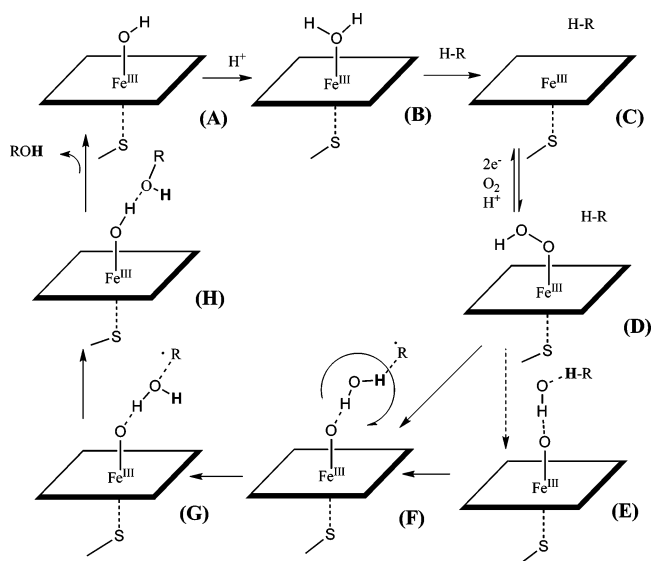


Figure 8. The postulated sequence of steps for the oxidation of hydrocarbons by cytochrome P450. The primary oxidizing agent is represented by MIN-10, for the oxidation of methane (Figure 9) and for the oxidation of isobutane (Figure 11). The existence of **E** as a long-lived intermediate is questionable. The square represents the heme bound to the enzyme.

(d) The Hydroxylation Step in Cytochrome P450 Oxidation of Methane. Early theoretical studies by Harris, Loew,^{9a,b} and Yoshizawa^{9c,d} and their colleagues clearly demonstrated that DFT calculations on porphyrin iron hydroperoxides were feasible. There have also been numerous theoretical calculations by Shaik and his group,¹⁰ which, while supporting the ferryl oxygen species Cpd I as the primary oxidant, also provided valuable guidelines as to how such calculations can be most efficiently carried out. Many of the details of our own calculations were gleaned from careful examination of the methods used by these pioneering groups. The “two-state reactivity”¹⁰ model proposed by Shaik is now generally accepted by many with the exception of the “two-oxidant” proponents.⁴

We are currently operating under the assumption that the oxidizing capacity of P450 arises from the participation of a low-lying transient hydroperoxide species resulting from O–O bond rearrangement in much the same manner as postulated for the metastable species derived from GS peroxyxynitrous acid (Figure 1, TS-1).¹⁸ Further support for the intervention of a metastable hydroperoxide form (MO••••HO) comes from the observation that the activation barrier for HO–ONO* C–H oxidation in methane is up to 15 kcal/mol lower on this open-shell metastable PES^{18b} than the corresponding oxidation on the closed shell surface. We have used the mechanism for isobutane hydroxylation by [HO••••ONO*]^{18b} as a template for this new reaction pathway for P450 oxidation because it appeared to follow quite logically after we located a discernible metastable isomeric state of iron hydroperoxide **5**. Although it is known that the hydrocarbon substrate enters the reactive site prior to formation of the FeO–OH, we initiated this preliminary surface (Figure S9 in Supporting Information) with methane weakly hydrogen bonded to the inverted distal oxygen of MIN-10 (FeO••••HO*). We also assumed, initially, that this is a two-step process involving a hydrogen abstraction followed by a hydroxylation or rebound step (Figure S10).

The H-bonding distance in H-bonded complex Min-19a is 2.6 Å (Figure 9). While the doublet surface is quite often lower

(26) Harris, D. L.; Loew, G. H. *J. Am. Chem. Soc.* **1998**, *120*, 8941.

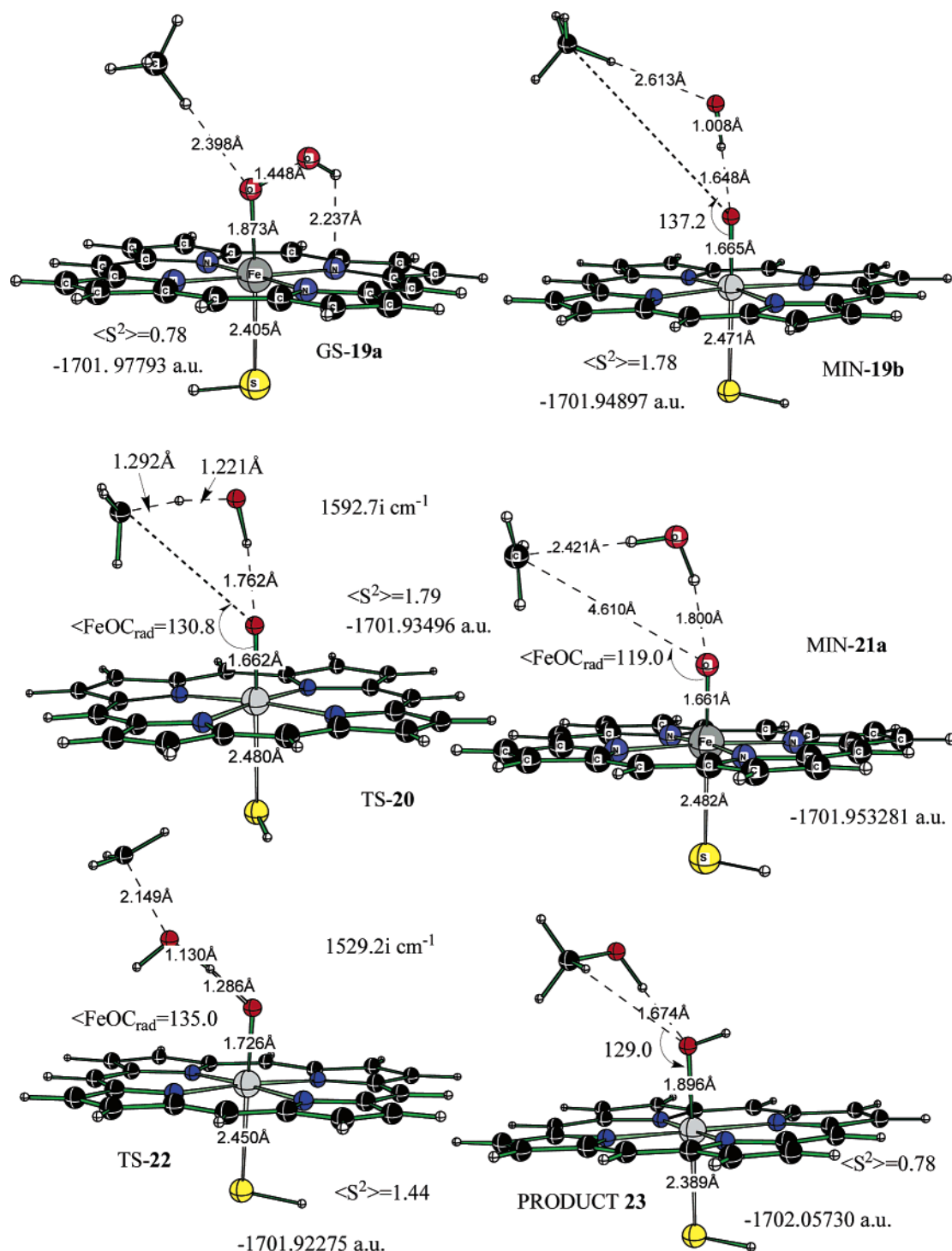


Figure 9. B3LYP-optimized stationary points on the PES for the oxidation of methane to methanol with primary oxidant MIN-10 (PorFe(SH)O \cdots HO). The 6-311+G(d,p) basis set was used for both oxygen atoms.

in energy than the quartet, the quartet-TS for hydrogen abstraction from methane (TS-20) is identical in total energy to the doublet, while the barrier for the quartet hydroxylation step (TS-22) is 7.7 kcal/mol higher in energy (Figure 10). The barrier for the hydrogen abstraction from methane by complex MIN-10 is only 8.8 kcal/mol. Hydrogen bonding of the \bullet OH radical to the ferryl oxygen in MIN-10 tempers its reactivity, as evidenced by the fact that the activation barrier for hydrogen abstraction from methane by the \bullet OH radical itself is only 2.3 kcal/mol.^{18b} The corresponding barrier for the [Fe^V=O]

H-abstraction from methane, starting from the ferryl oxygen (Cpd I) reported by Shaik,^{10c} is 26.5 kcal/mol. This does not include any energy requirements for forming Cpd I (eq 1). Thus, it might appear that the reactivity of the hydroxyl radical in MIN-10 is much greater than that of the ferryl oxidant in Cpd I. However, the oxidation of the primary C–H in methane should exhibit a significant overall barrier by either oxidant (MIN-10 or Cpd I) relative to the GS FeO–OH complex, GS-19a (Figure 9). Indeed, we calculate a barrier for a concerted H-abstraction step, relative to GS-19a, of 27.0 kcal/mol

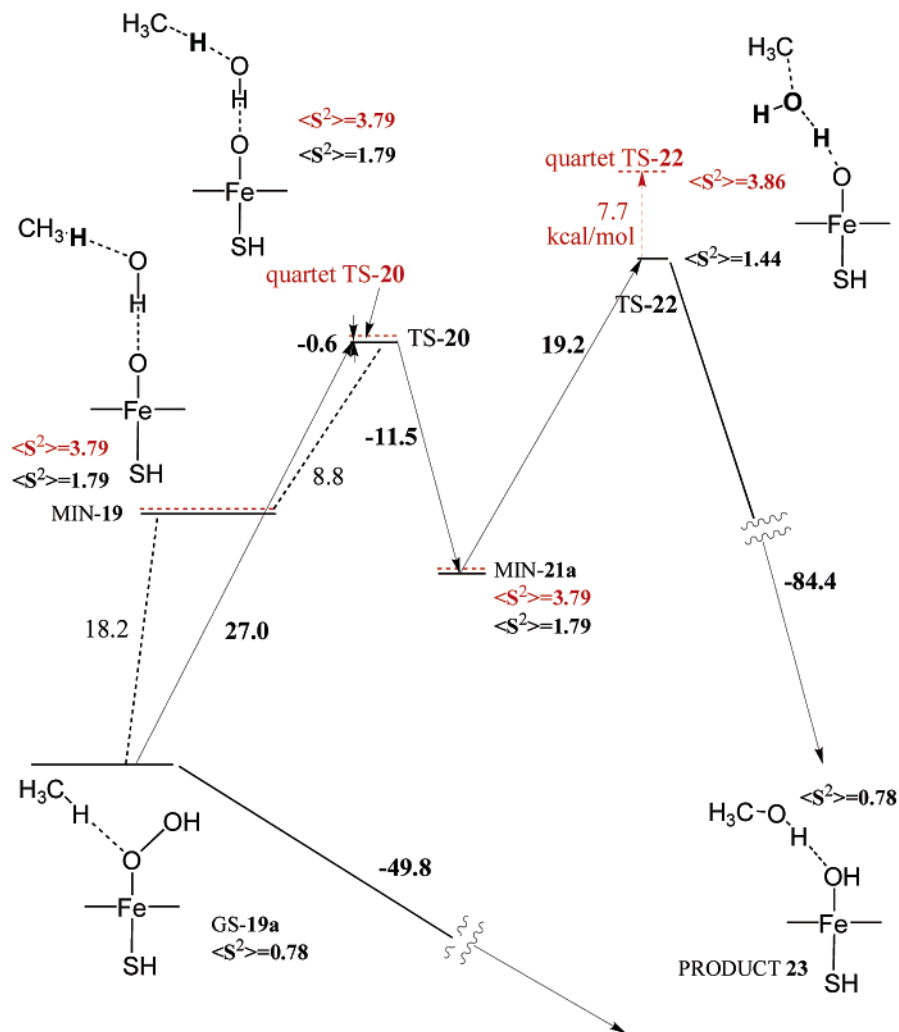


Figure 10. Energy diagram (kcal/mol) for the oxidation of the methane with **10** (PorFe(SH)O...HO). Numbers in black are calculated for the doublet states; red numbers correspond to quartet states.

(comparable to that for Cpd I)^{10c} and an overall activation barrier for the hydroxylation of methane of 34.6 kcal/mol (Figure 10). Thus, the hydrogen abstraction step by Cpd I exhibited an overall calculated barrier 10 kcal/mol lower in energy,^{10c} provided that the formation of Cpd I had a negligible activation barrier and that hydrogen abstraction by Cpd I was the rate-limiting step. This point is addressed in detail for isobutane hydroxylation below.

The structure for the transition state involving H-abstraction from methane by bound hydroxyl radical MIN-10 is about what was expected, and, while the structure was comparable to that observed for hydroxyl radical itself attacking isobutane,^{18b} the reactivity was diminished due to the H-bonding interaction with the ferryl oxygen. In TS-20, the departing hydrogen atom is almost equidistant between the carbon atom and the developing water molecule. The Fe–O and Fe–S distances in abstraction TS-20 are 1.66 and 2.48 Å. In both TS-20 and hydroxylation TS-22, the magnitude of the single imaginary in each TS is quite high ($>1500i$ cm⁻¹), indicative of a TS dominated by the transfer of a light hydrogen atom. Animation of the imaginary frequency in H abstraction TS-20 shows that it is comprised solely of transfer of the hydrogen atom from methane to the HO• fragment to form an H-bonded water molecule. The reaction vectors in

hydroxylation TS-22 are due largely to transfer of the hydrogen from the water molecule to the ferryl oxygen with a small contribution of the rebound motion of the hydroxyl radical to the methyl radical coming after the barrier is crossed. The overall oxidation process to produce methanol H-bonded to the Fe–OH group of the heme (PRODUCT-23) is exothermic by 49.8 kcal/mol (Figure 10). This final product and intermediate **21b** (Figure S9) appear to be the only structures on this PES that are close to pure doublets. Recall that MIN-10, in the absence of the methane fragments, has nearly identical energies for the doublet and quartet states.

However, this mechanistic picture is further complicated by the fact that we have located several intermediates potentially following H-abstraction TS-20 (Figure 9). First, the expectation values of the S^2 operator ($\langle S^2 \rangle = 1.78$ and 1.79) for both MIN-19b and TS-20 suggest a significant contamination of the doublet wave function with quartet character. Intermediate **21b** (Figure S10), a pure doublet, is 15.7 kcal/mol higher in energy and **21a**, with $\langle S^2 \rangle = 1.79$, is 11.5 kcal/mol lower in energy than TS-20 (Figure 10). Second, it appears that the quartet contribution to the wave function results in a net stabilization. Because the doublet structures are more typically lower in energy than the corresponding quartets, we will assume an

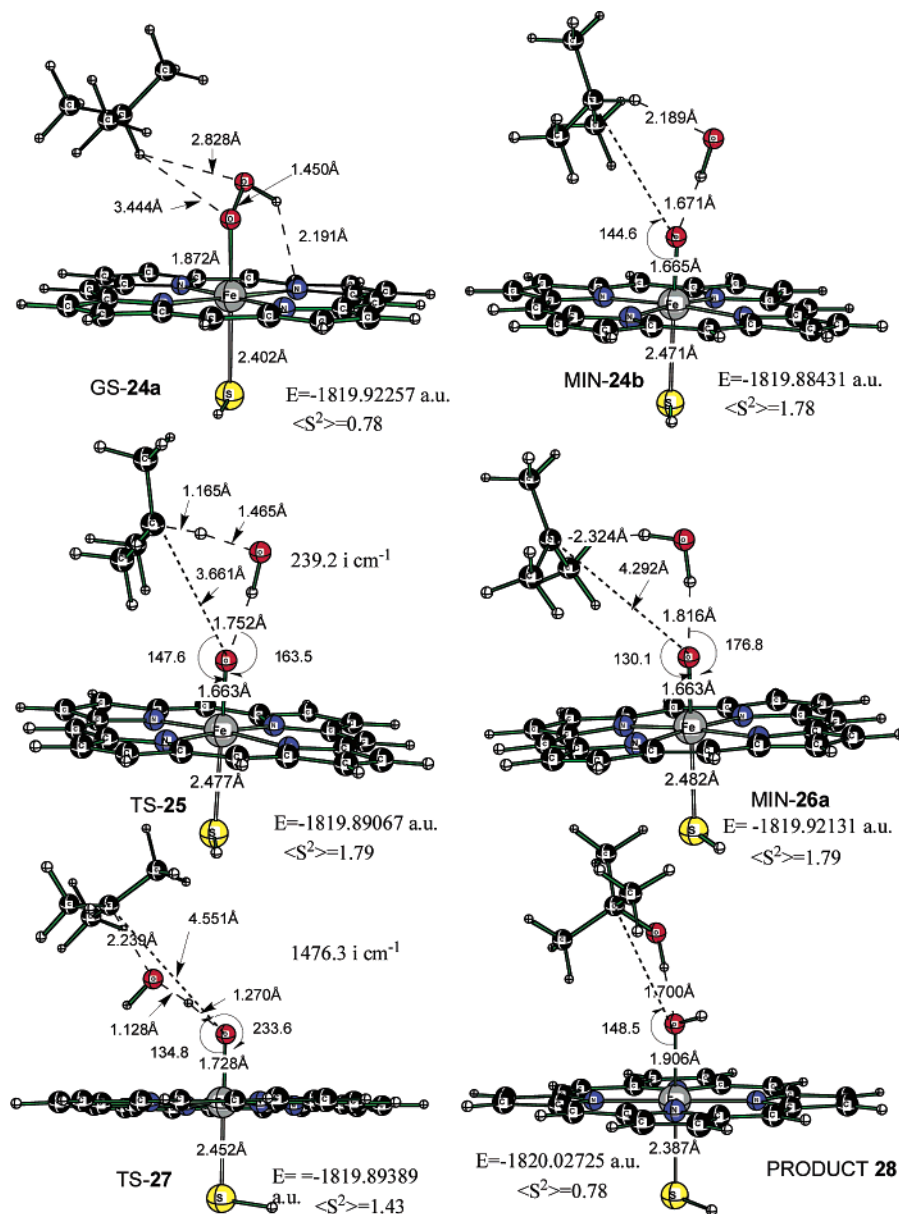


Figure 11. B3LYP-optimized stationary points for the oxidation of isobutane to *tert*-butyl alcohol with primary reactant **10** (PorFe(SH)O \cdots HO). All of the atoms directly involved in the oxidation step (OOH and C–H) were treated with the 6-311+G(d,p) basis set. The total number of the basis functions and primitive Gaussians in this reaction system are 413 and 935, respectively. We also located MIN-26b structure with $\langle S^2 \rangle = 1.79$ and $E = -1819.90807$ au.

oxidation sequence on the doublet PES with selected relative energies given for the corresponding quartet states when available.

An important question that remains for this methane PES is whether this is a two-step reaction or a concerted but nonsynchronous process. As noted above, we have located an intermediate **21a** that is 11.5 kcal/mol lower in energy than TS-20, and this would require a 19.2 kcal/mol activation barrier for the second hydroxylation step (TS-22). However, the geometry of intermediate **21a** is such that a bending motion of the water molecule through an angle of $\sim 70^\circ$ would be required to present the oxygen atom at the proper angle for formation of the C–OH bond in TS-22 and complete the hydroxylation step. This potential heavy atom motion for the isobutane oxidation surface will be addressed further below. At this point, we suggest that TS-20 and TS-22 may be connected to a shallow minimum (not

located) or this could potentially be a continuing nonsynchronous surface.

(e) The Hydroxylation Step in Cytochrome P450 Oxidation of Isobutane. The series of steps for the oxidation of methane (Figure 8) by model oxidant **10** provide both TSs and intermediates consistent with the intervention of a transient hydroperoxide that is comprised of a hydrogen-bonded hydroxyl radical. However, the tertiary C–H bond in isobutane provides a more realistic substrate for hydroxylation (Figures 11 and 12). Location of a pre-reaction complex for isobutane is difficult because the bonding interactions are quite weak and the molecular assembly is very floppy. The H-bonding H \cdots O distance in ground-state pre-reaction complex GS-24a (Figure 11) is 2.8 Å. The rearranged FeO–OH hydrogen-bonded complex MIN-24b was 24.0 kcal/mol higher in energy than GS-24a. We immediately observed a significant difference between

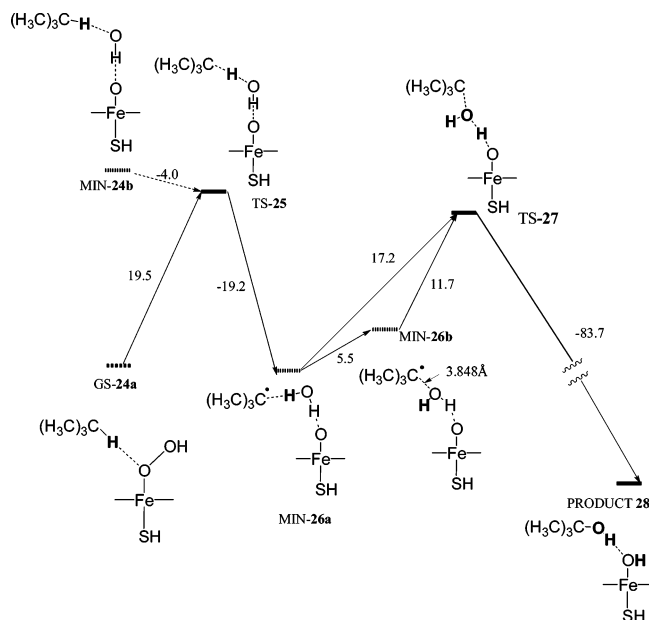


Figure 12. Energy diagram (kcal/mol) for the oxidation of the isobutane with ground state, **24a** (GS-8 hydrogen bonded to isobutane). MIN-24b [model oxidant MIN-10 (PorFe(SH)O \cdots HO) hydrogen bonded to isobutene] is not necessarily on the reaction pathway.

this PES and the one described above for the hydroxylation of methane. The activation barrier for H-abstraction from isobutane is only 19.5 kcal/mol (TS-25). The isobutane doublet PES has the TS for hydrogen abstraction (TS-25) 4.0 kcal/mol lower in energy than hydrogen-bonded complex MIN-24b (Figure 11). This strongly implies that the hydrogen abstraction from isobutane is a concerted process that does not necessarily involve the rearranged hydrogen peroxide (FeO \cdots HO) as a discrete intermediate preceding the H abstraction step. It also appears that the presence of the hydrocarbon serves to lower the barrier for the FeO–OH isomerization step because the gas-phase activation barrier for the somersault motion is 24.3 kcal/mol (TS-9, Figure 6) in the absence of the hydrocarbon. This is quite consistent with conventional wisdom because the altered overall pathway described by Figure 8 clearly indicates that the substrate must be bound at the active site *prior* to the two-electron reduction step (C \rightarrow D, Figure 8) attending the formation of the iron hydroperoxide moiety (FeO–OH, Cpd 0).¹

As noted above, the TS for hydrogen abstraction on the quartet surface is again almost identical in total energy to that on the doublet surface. This does not appear to be a problem with spin contamination of the wave function because both structures have comparable values of $\langle S^2 \rangle$ close to 1.75 that are also consistent with TS-20 on the methane PES. This is very likely a problem associated with the DFT method because we are unable to locate a TS for hydrogen abstraction from isobutane with hydroxyl radical itself. With the B3LYP/6-311+G(d,p) basis set, the combined total energies of the reactants (isobutane + \bullet OH) were always higher in energy than the structure resembling the TS. We were able to locate hydrogen abstraction TSs for this H abstraction reaction at both the MP2/6-31+G(d,p) ($\Delta E^\ddagger = 2.6$ kcal/mol) and the QCISD/6-31G(d) levels ($\Delta E^\ddagger = 7.2$ kcal/mol, see Table S7 in the Supporting Information).

We do see a similarity in both methane and isobutane surfaces in that the hydrocarbon fragment does not move very much

along the reaction coordinate, maintaining its position with respect to the Fe–O bond with an Fe–O–C angle of about $140^\circ \pm 10^\circ$ (Figure 11). Consistent with the basic concept of reduced mass that only the lighter atoms move in a transition state, the single imaginary frequency for TS-25 ($\nu = 239.2i$ cm^{-1}) has the OH fragment pivoting about the ferryl oxygen to abstract the H atom from isobutane with very little motion of the larger isobutane molecule. In contrast, TS-20 (Figure 9) for hydrogen abstraction from methane had a much larger imaginary frequency that was consistent with only the lighter hydrogen atom moving in a ping-pong motion between the hydroxyl oxygen and the methyl carbon. The second TS that transfers the hydrogen atom back from the water molecule to the ferryl oxygen (TS-27, $\nu = 1476.3i$ cm^{-1}) is again almost exclusively comprised of the H atom transfer step with a minor component of the OH rebound to form the C–O bond of the *tert*-butyl alcohol product. We again question whether the water complex bound to the ferryl oxygen and the *tert*-butyl radical (MIN-26a and MIN-26b, Figure S11 in the Supporting Information) is actually a discrete minimum on the reaction surface.

As shown in Figure 11, the Fe–O–H angle to the water molecule in TS-25 is 163.5° , and in TS-27, for the hydroxylation step, this angle has increased to 233.6° . Thus, the developing water molecule must swing through an angle of $\sim 70^\circ$ to present the carbon radical face at the proper angle to the incipient \bullet OH radical for the rebound step to form *tert*-butyl alcohol. In general, the C–O–H angle in the TS for hydroxylation (102°) must be about the same as that of the final angle in the alcohol product (109°). Examination of intermediate **26a** shows that the carbon fragment is too close to the plane of the porphyrin ring to allow the requisite motion of the water molecule for this second TS unless there is the heavy atom motion of the isobutane fragment. Moreover, the closeness of the hydrocarbon to the heme nitrogens has resulted in a lowering of the total energy of MIN-26a to a point where if it were connected to TS-27 then the barrier of the second TS from this intermediate would be relatively high ($\Delta E^\ddagger = 17.2$ kcal/mol). We also attempted to locate the minimum preceding the hydroxylation step, TS-27, with the oxygen atom of the water molecule pointed toward the carbon radical center. Although somewhat higher in energy (5.5 kcal/mol), MIN-26b (Figure 12) has the *tert*-butyl radical drifting far away from the water molecule (3.85 Å), a situation that would never be tolerated in the fairly tight local environment of the active site. Both MIN-26a and MIN-26b (Figure S11) are discrete minima, but only MIN-26b has the proper orientation of the incipient C–O bond for the rebound hydroxylation step in TS-27. Because the difference in total energy of TS-25 and TS-27 is only 2.0 kcal/mol, with the latter TS being lower in energy it is tempting to assume, as above for the methane surface, that these TSs are connected by a very shallow minimum on what is ostensibly a concerted but nonsynchronous pathway.

Because we did not observe an activation barrier for H-abstraction with HO \bullet for isobutane itself at the DFT level, the highest point on this isobutane PES is the TS for the somersault motion of the hydroperoxide (in the presence of isobutane) to produce TS-25 ($\Delta E^\ddagger = 19.5$ kcal/mol). By comparison, in a related study, Yoshizawa^{9c,d} reported a barrier for abstraction of the 2° C–H at C5 in camphor by the ferryl oxygen of Cpd I (doublet) of 23.8 and 28.6 kcal/mol for C–H bond cleavage

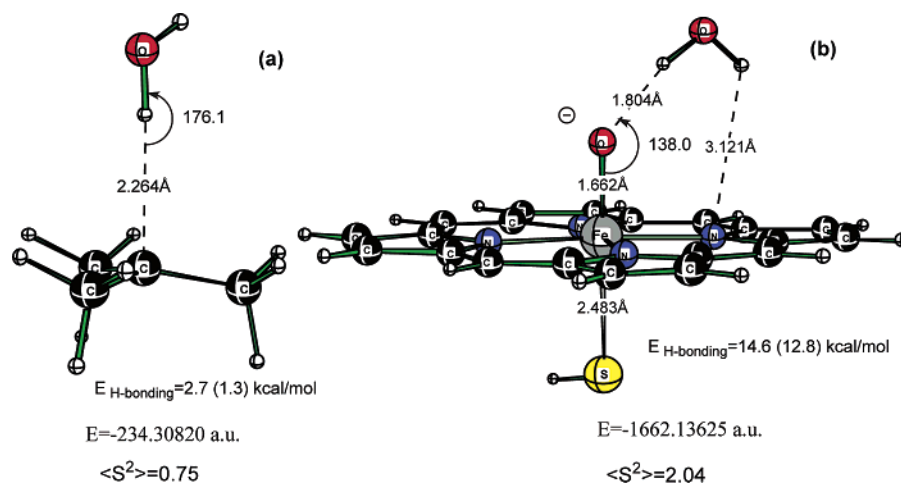
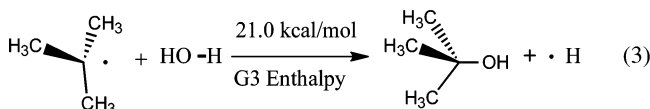
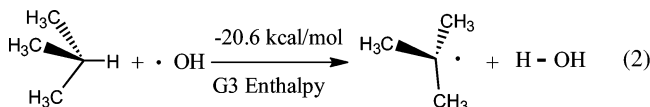


Figure 13. B3LYP-optimized complexes of (a) water with *tert*-butyl radical and (b) water with Por(SH)FeO anionic triplet. Complex (a) is fully optimized at the UB3LYP/6-311+G(d,p) level. In complex (b), the 6-311+G(d,p) basis set is used for the oxygen atoms and two water hydrogens; all other atoms (except Fe) are treated with the 6-31G basis set. Energy of H-bonding in parentheses is calculated with zero-point vibrational energy corrections.

in ethane. Thus, in the present study, the ferryl bound hydroxyl radical appears to be more effective than Cpd I for C–H bond cleavage.

The overall hydroxylation of isobutane is an extremely exothermic oxidation reaction ($\Delta E = 65.7$ kcal/mol) when mediated formally by the weakly bound hydroxyl radical in intermediate **10**. The abstraction of a hydrogen atom from isobutane by hydroxyl radical itself, to produce a water molecule, is attended by the liberation of 20.6 kcal/mol (eq 2). Contrariwise, the hydroxylation of *tert*-butyl radical by a water molecule is essentially equally endothermic (eq 3). This makes



it obligatory that the hydroxylation step in TS-27 be attended by the concerted transfer of a hydrogen atom from water to the ferryl oxygen as suggested by the magnitude of the single imaginary frequency as discussed above. The water molecule is only weakly H-bonded (2.7 kcal/mol) to the *tert*-butyl radical as shown in Figure 13. When the oxygen is aimed at the radical center (as required for the hydroxylation step), the distance between the fragments increases dramatically and the stabilization energy is only 0.15 kcal/mol.^{18b} These observations support the contention that the local environment of the active site and its steric demands play a major role in constraining the reactants to be close together in this hydroxylation reaction.

As suggested above, one of the primary functions of the cysteinate residue is to increase the basicity of the ferryl oxygen to facilitate the concerted nature of the transfer of a hydrogen atom from water back to the ferryl oxygen in the TS-27 for the hydroxylation step, the binding energy of a water molecule to the anionic heme is 14.6 kcal/mol (Figure 13).

(f) The Overall Reaction Pathway for Cytochrome P450.

In summary, we suggest a modified overall pathway for the

P-450 hydrocarbon oxidation step (Figure 8) involving the model transient hydroxyl radical bound iron heme **10**. Several key factors alluded to above have led us to this conclusion. The O–O BDE for the porphyrin FeO–OH **5** was only 22.9 kcal/mol, suggesting the possibility of this unique transformation producing a metastable isomeric hydroperoxide. The activation energy for the OH somersault process is 19.7 kcal/mol, and the H-bonded minimum is only 16.4 kcal/mol above the GS FeO–OH **5** (Figure 3). The proton affinity (PA) of the distal oxygen in FeO–OH in **8** is estimated to be 40 kcal/mol less than the proximal oxygen, belying the probability of distal protonation and formation of a ferryl oxygen intermediate (eq 1). When the axial sixth SH[−] ligand was included, the basicity of the complex increased and H-bonded hydroxyl radical **10** was found to be 17.5 kcal/mol above GS hydroperoxide **8** stabilized by a considerable hydrogen-bonding energy (17 kcal/mol, Figure 6). Because the O–O BDE of **8** is calculated at this same level to be 31.7 kcal/mol, the HO• radical in MIN-**10** is bound by 14 kcal/mol and should not exhibit the notorious indiscriminate reactivity of a free hydroxyl radical. The overall activation energy for the concerted hydroxylation of isobutane to produce *tert*-butyl alcohol is only 19.5 kcal/mol. These combined factors suggest to us that the basic mechanism suggested in Figure 8 involving a hydrogen-bonded hydroxyl radical has merit and is worthy of further consideration as the approximate enzymatic pathway for P450 hydroxylation.

The reaction pathway outlined in Figure 8 suggests that at the beginning of a new catalytic cycle, as the protein unfolds and an incoming substrate binds to the enzymatic site, *water from bulk solvent* protonates the Fe–OH center (**A**) to form the resting state **B** and introduces the hydrocarbon substrate with the displacement of the water molecule producing **C**. The proton affinity of anionic hydroxyl complex **A** is 344.3 kcal/mol (Figure 5), a value 9 kcal/mol greater than the PA of the proximal oxygen in the initial anionic FeO–OH complex **8**. We suggest that FeO–OH adduct **D** (Cpd 0) is a discrete intermediate that is stabilized by a hydrogen-bonding interaction with Thr-252 because this appears to be the most generally accepted portion of the overall sequence. X-ray studies^{7,8} on P450_{cam} indicate the presence of Cys³⁵⁷ during formation of Cpd 0. The barrier for isomerization of the FeO–OH group in **8**, in the presence

of the thiolate (TS-9, $\Delta E^\ddagger = 24.3$ kcal/mol), is higher than the barrier for concerted C–H cleavage (TS-25, $\Delta E^\ddagger = 19.5$ kcal/mol), strongly supporting a concerted but nonsynchronous pathway involving the formation of isomeric $\text{FeO}\cdots\text{HO}$ (**E**). The hydrogen abstraction step producing a structure resembling **F**, but not necessarily as a discrete intermediate, with a nonsynchronous hydroxylation step designated by **G**, appears to be the best pathway to produce product alcohol hydrogen-bonding to the resting state, **H**, that we can suggest based upon our limited calculations at this time. There is a considerable amount of experimental data that is consistent with this modified reaction sequence, as we will outline in a future paper.

3. Computational Details

Quantum chemistry calculations were carried out using the Gaussian98 and Gaussian03 programs²⁷ system utilizing gradient geometry optimization.²⁸ Calculations were performed using the UB3LYP hybrid density functional²⁹ in combination with the Los Alamos effective core potential coupled with a double- ζ LANL2DZ basis set³⁰ for iron, an all-electron 6-311+G(d,p) basis set for oxygen, and 6-31G basis set for the rest of the atoms. In Figures 3 and 6, the 6-311+G(d,p) basis set was also added to the hydrogen of OOH as indicated in bold type. We used a 6-31G basis set for carbon atoms, and the iron used the LANL2DZ ECP²¹ except as noted above when we also increased the basis set size on Fe and N. The GEN (allows different user-specified basis sets for different atoms to be used) and PSEUDO=READ (requests that a model potential, LANL2DZ, be substituted for the core

electrons) keywords have been used to perform these calculations in utilizing the Gaussian program. For the isobutane oxidation sequence (Figure 11), the 6-311+G(d,p) basis set was applied additionally to the tertiary carbon and hydrogen C–H bond involved in the abstraction and rebound steps, as well as the OOH fragment. A similar approach has proven to be qualitatively reliable and of similar performance to higher level basis sets or methods.^{10d,31} Calculations on the smaller models (**11–18**) were performed with the 6-311+G(d,p) basis set on all atoms except Fe (where the effective core potential coupled with a LANL2DZ basis set was used). In **17** and **18**, the planarity of the four-nitrogen array in the porphyrin was maintained by a fixed dihedral angle $-\text{NNNN} = 0.0$. G3 calculations³² have been performed for eqs 2 and 3. The reaction of $\bullet\text{OH}$ radical with isobutane was also studied using MP2 and QCISD methods.

Cpd 0 iron hydroperoxide (**8**, Figure 6) was modeled as an iron-peroxo complex, where the axial thiolate ligand was truncated to SH. This was established as a sufficient model in previous studies by Shaik.^{10d} All structures were fully optimized, followed, in essentially all cases, by complete frequency analyses for the doublet and quartet spin states.

Acknowledgment. This work was supported by the National Science Foundation (CHE-0138632), partially supported by the National Computational Science Alliance under CHE050085 and CHE050039N, and utilized the NCSA IBM P690 and NCSA Xeon Linux Supercluster.

Supporting Information Available: Total energies, Cartesian coordinates, and CASSCF orbitals. Complete list of authors for ref 27. This material is available free of charge via the Internet at <http://pubs.acs.org>.

JA052111+

- (27) (a) Frisch, M. J.; et al. *Gaussian 98*, revision A.7; Gaussian, Inc.: Pittsburgh, PA, 1998. (b) *Gaussian 03*, revision B.05 (SG164-G03RevB.05); Gaussian, Inc.: Pittsburgh, PA, 2003. See the Supporting Information for the full list of authors.
- (28) (a) Schlegel, H. B. *J. Comput. Chem.* **1982**, *3*, 214. (b) Schlegel, H. B. *Adv. Chem. Phys.* **1987**, *67* (Pt. 1), 249. (c) Schlegel, H. B. In *Modern Electronic Structure Theory*; Yarkony, D. R., Ed.; World Scientific: Singapore, 1995; p 459.
- (29) (a) Becke, A. D. *Phys. Rev. A* **1988**, *38*, 3098. (b) Becke, A. D. *J. Chem. Phys.* **1993**, *98*, 5648. (c) Lee, C.; Yang, W.; Parr, R. G. *Phys. Rev. B* **1988**, *37*, 785.
- (30) (a) Hay, P. J.; Wadt, W. R. *J. Chem. Phys.* **1985**, *82*, 270. (b) Wadt, W. R.; Hay, P. J. *J. Chem. Phys.* **1985**, *82*, 284. (c) Hay, P. J.; Wadt, W. R. *J. Chem. Phys.* **1985**, *82*, 299.

- (31) (a) Schoneboom, J. C.; Cohen, S.; Lin, H.; Shaik, S.; Thiel, W. *J. Am. Chem. Soc.* **2004**, *126*, 4017. (b) Schoneboom, J. C.; Lin, H.; Reuter, N.; Thiel, W.; Cohen, S.; Ogliaro, F.; Shaik, S. *J. Am. Chem. Soc.* **2002**, *124*, 8142. (c) Johansson, M. P.; Sundholm, D.; Gerfen, G.; Wikström, M. *J. Am. Chem. Soc.* **2002**, *124*, 11771. (d) Johansson, M. P.; Sundholm, D. *J. Chem. Phys.* **2004**, *120*, 3229.
- (32) Curtiss, L. A.; Raghavachari, K.; Redfern, P. C.; Rassolov, V.; Pople, J. A. *J. Chem. Phys.* **1998**, *109*, 7764.